Isolation and Identification of Residues of 4″-(*epi*-Methylamino)-4″-deoxyavermectin B_{1a} Benzoate from the Surface of Cabbage

Christopher L. Wrzesinski,*,† Byron H. Arison,‡ Jack Smith,§ Deborah L. Zink,§ William J. A. VandenHeuvel,‡ and Louis S. Crouch†

Department of Drug Metabolism II, Pesticide Metabolism and Environmental Safety Group, Merck Research Laboratories, P.O. Box 450, Three Bridges, New Jersey 08887, and Department of Drug Metabolism II and Department of Natural Products Chemistry, Merck Research Laboratories, P.O. Box 2000, Rahway, New Jersey 07065

Cabbage was treated with a single application of [^{14}C]-MK-0244, a semisynthetic avermectin analogue, at 0.3 lb/acre and harvested 1 day after application. The wrapper leaf and exterior head surface of the cabbage were rinsed with methanol, and 12 degradates were isolated from this rinse and identified by structural analysis. Ten of these residues can be accounted for by six previously reported transformations and two are apparently formed by novel transformations. This represents the first time that avermectin residues isolated from a plant have been unequivocally identified by direct methods. The cabbage residue profile bears a strong resemblance to that seen in the photodegradation of MK-0244 thin films on glass.

Keywords: *Avermectin; photodegradation; cabbage; surface residue; plant residue; pesticide*

INTRODUCTION

Avermectins are macrolides produced by the soil actinomycete *Streptomyces avermitilis*. The naturally occurring abamectin and the semisynthetic ivermectin are currently marketed as crop protection or as animal health products. Ivermectin is active against endo- and ectoparasites in both livestock and companion animals. Abamectin (B_1) is primarily a miticide and is currently sold for use on ornamentals, cotton, and selected fruit and vegetable crops. It is also used to treat endo- and ectoparasites in cattle. A semisynthetic abamectin analogue, 4″-(*epi*-methylamino)-4″-deoxyavermectin B_1 benzoate (MK-0244, emamectin benzoate), is currently being developed to control Lepidopteran insects on a number of crops including cole and lettuce. Like ivermectin and abamectin, MK-0244 is a mixture of two avermectin homologues, >90% 4″-(*epi*-methylamino)-4″-deoxyavermectin B_{1a} (MAB1a) and <10% 4″-(*epi*-methylamino)-4″-deoxyavermectin B_{1b} (MAB1b) (see Figure 1).

This paper describes the isolation of MAB1a residues from cabbage and their identification by nuclear magnetic resonance (NMR) and mass spectrometric analysis (MS). Additionally, other residues were characterized by chromatographic retention times and by UV absorption spectra. The results reported here represent the first time avermectin residues isolated from plants have been unequivocally identified. The extreme complexity of the residue profile is also demonstrated.

MATERIALS AND METHODS

MAB1a and Derivatives. Radiolabeled MAB1a was supplied by Merck Research Laboratories (MRL), Labeled Compound Synthesis, Rahway, NJ. Nonradiolabeled MK-0244 was supplied by MRL, Department of Drug Metabolism II. Emulsifiable concentrate (EC) was supplied by the Merck Agricultural Research Department, Three Bridges, NJ. [^{14}C]MAB1a benzoate (>97% radiochemical purity, specific activity 29.0 μCi/mg), in which the ^{14}C label was located at the C3, C7, C11, C13, or C23 position (one position per molecule, see Figure 1)

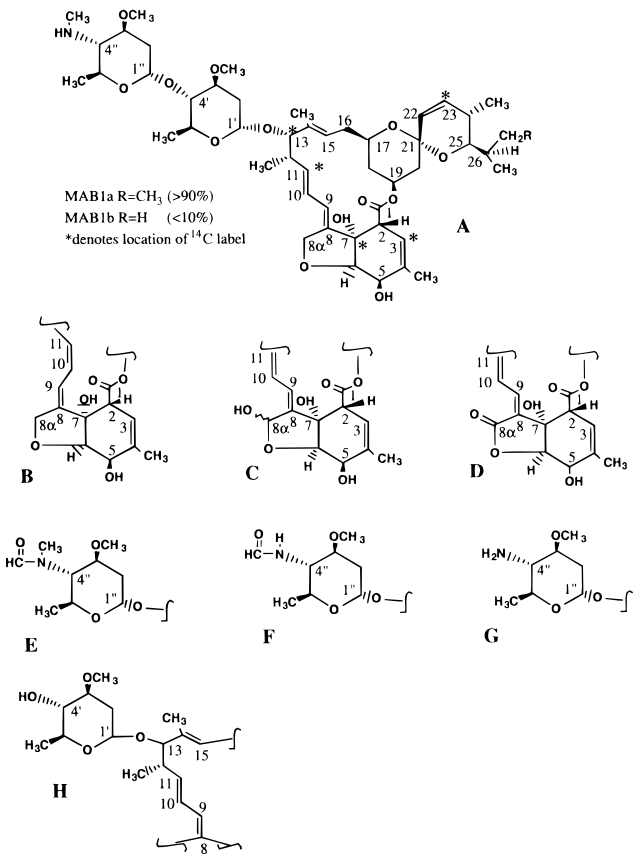

Figure 1. Structures of MK-0244 (A) and related residue standards 8,9-*Z*-MAB1a (B), 8α-OH-MAB1a (C), 8α-oxo-MAB1a (D), MFB1a (E), FAB1a (F), AB1a (G), and MSB1a (H).

* Author to whom correspondence should be addressed.

† Merck Research Laboratories, Three Bridges.

‡ Department of Drug Metabolism II, Merck Research Laboratories, Rahway.

§ Department of Natural Products Chemistry, Merck Research Laboratories, Rahway.

0021-8561/96/1444-0304$12.00/0

(Ku et al., 1984), and nonradiolabeled MK-0244 were dissolved together in EC, and this was diluted with water to give an application solution of 1313 mg/L (6.9 μCi/mg MK-0244).

Along with MAB1a the following seven MAB1a derivatives were also supplied by MRL as reference standards: 8,9(*Z*)-4″-deoxy-4″-(*epi*-methylamino)avermectin B_{1a} (8,9-*Z*-MAB1a), 8α-hydroxy-4″-deoxy-4″-(*epi*-methylamino)avermectin B_{1a} (8α-OH-MAB1a), 8α-oxo-4″-deoxy-4″-(*epi*-methylamino)avermectin B_{1a} (8α-oxo-MAB1a), 4″-deoxy-4″-(*epi*-*N*-formyl-*N*-methyl)-avermectin B_{1a} (MFB1a), 4″-deoxy-4″-*epi*-*N*-formylavermectin B_{1a} (FAB1a), 4″-deoxy-4″-*epi*-aminoavermectin B_{1a} (AB1a), and avermectin B_{1a} monosaccharide (MSB1a) (see Figure 1).

Instrumentation. High-performance liquid chromatography (HPLC) was performed using two different systems. System 1 consisted of a Perkin-Elmer Model 250 binary pump with a Perkin-Elmer 1020 integrator and a Spectra Physics 8480-010 UV detector. Wavelength was continuously monitored at 245 nm. System 2 consisted of a Spectra Physics Model 8700 gradient controller and an HP Model 1040A diode array detector attached to an HP 85B computer. Wavelength was continuously monitored from 210 to 400 nm, and UV absorption spectra of individual peaks at 210, 245, and 280 nm were automatically taken. Pharmacia Frac-100 fraction collectors were used with both systems to collect 1 min eluate fractions (either 1 or 3 mL) in Packard 6 mL plastic pony vials. Rheodyne 7125 injectors and Brownlee guard columns (RP or NP as appropriate) were also used for both systems.

Proton nuclear magnetic resonance (NMR) analysis was performed at 400 MHz using a Varian Unity 400 spectrometer and at 500 MHz using a Varian Unity 500 spectrometer. In all cases the isolated residues were dissolved in $CDCl_3$ and analysis was run at room temperature using a 1 s acquisition time and a 45° flip angle.

Fast atom bombardment (FAB) mass spectrometry was performed using either a MAT 731 spectrometer with an acceleration voltage of 10 kV or a JEOL SX-102A spectrometer with an acceleration voltage of 3 kV. A xenon gas FAB gun was used in both cases. Samples were dissolved in methanol and analyzed in a matrix of 20:80 dithiothreitol/dithioerythritol (magic bullet). Exact mass measurements were made at high resolution with Ultramark 1960 (fomblin) as the reference. The electron impact spectra (EI) were obtained on a JEOL SX-102A (90 eV). Exact mass measurements were performed at high resolution using perfluorokerosine (PFK) as the internal standard.

Experimental Methods. A plot of 20 mature cabbage plants (Copenhagen market variety, *Brassica oleracea* L.) was treated with one application of [^{14}C]-MK-0244 at 20 times (0.3 lb of ai/acre) the normal use rate, and 10 plants were harvested 1 day after application. The wrapper leaf and exterior head surface of the cabbage were rinsed with methanol. The methanol rinse sample volume was first reduced under vacuum to 150 mL and then diluted with water to give a 70:30 methanol/water solution. An initial fractionation was performed using Varian (Harbor City, CA) Mega-Bond Elut C_{18} solid phase extraction (SPE) cartridges (6 cm^3, 1 g). Each cartridge was first conditioned by eluting 20 mL of methanol followed by 20 mL of water and finally 20 mL of 70:30 methanol/water (volumes approximate). Next, 7 mL of the sample in 70:30 methanol/water was applied to each SPE cartridge followed by a rinse with 35−40 mL of 70:30 methanol/water. The residues contained in this eluate were termed "polar" because all were found to elute before the monosaccharide (MSB1a), the most polar of the available standards, using reversed phase HPLC (see Figure 2a). This fraction comprised 9.6% of the recovered radioactivity.

The cartridges were then eluted with 20−25 mL each of methanol. This eluate (61.4% of recovered radioactivity) was termed the "nonamine" fraction as it contained avermectin-like residues in which the amine functionality either was missing or was modified so that a basic proton was no longer present.

Finally, the cartridges were eluted with 25−30 mL each of methanol and 5 mM ammonium acetate. This eluate (29.1% of recovered radioactivity) was termed the "amine" fraction as it contained avermectin-like residues with the amine group either unchanged or still having a basic proton. Residues possessing a basic proton are apparently retained on the cartridge until secondary interactions are disrupted by a modifier such as ammonium acetate. Overall recovery for the solid phase extraction averaged 79.2%.

The residues from the nonamine and amine fractions were subsequently resolved or partially resolved using an Axxiom C_{18} semipreparative column and either HPLC method 1A or 2 (Table 1), respectively, and collecting 1 min fractions. Seven injections were required to fully fractionate the nonamine sample, and four were required to fractionate the amine sample. Representative chromatograms for both of these fractions are given in Figure 2b,c. Initial peak identifications were made by comparison with retention times of authentic MAB1a derivative standards. These standard retention times were also used as points of reference in work with unknown peaks or regions between peaks.

Residue peaks and areas between peaks which were obtained by semipreparative HPLC (as determined by UV and radiochromatography) were then separated into individual residues using a combination of HPLC methods and columns as detailed in Table 2. Before any HPLC analysis, the fractions of interest were combined and taken to dryness *in vacuo* or under a stream of nitrogen and then reconstituted in the appropriate starting mobile phase. Because of the large number of residues present, a total of 10 different HPLC methods and 4 different HPLC columns were used (Table 1).

The rinsed cabbage leaf was minced and then homogenized with approximately 1 mL of methanol/g of minced cabbage using a Brinkman Polytron. The homogenized cabbage was centrifuged and the pellet extracted two times with 1 mM ammonium acetate in methanol followed by three times with 5 mM ammonium acetate in 50:50 methanol/water. The combined supernatants were then placed in a freezer (−20 °C) overnight to precipitate natural products. This precipitate was combined with the extraction pellet. This combined pellet contained the total nonextractable residues and represented 4.7% of the total radioactive residues. The remaining supernatant and the methanol rinse contained the extractable residues and these represented 50.0% and 45.3%, respectively, of the total radioactivity (95.3% total extractable residues). The methanol rinse sample was calculated to contain 13 000 MAB1a benzoate μg equivalents.

HPLC and Ultraviolet (UV) Spectroscopy for Residue Characterization. Avermectins have characteristic UV absorption spectra which result from the 8,9 10,11 diene functionality. A change in the absorption spectrum is therefore diagnostic of a change at or near the diene functionality. This has been previously noted for both abamectin (Crouch et al., 1991) and MK-0244 (Feely et al., 1992). Therefore in many cases the UV absorption spectrum of an unknown residue as taken by photodiode array detection during HPLC analysis was important in characterizing and identifying that residue. The absorption spectrum of MAB1a is given in Figure 3A. Isomerization of the 8,9 double bond from the *E* configuration to the *Z* configuration as in 8,9-*Z*-MAB1a leads to a slight shift in the λ_{max} of the absorption spectrum as well as a change in the overall shape of the spectrum (Maynard, 1989) (Figure 3B). The extended conjugation of 8α-oxo-MAB1a leads to a bathochromic shift in the absorption spectrum to λ_{max} = 280 nm (Figure 3C). The 8α-OH-MAB1a residue has a UV absorption spectrum similar to that of MAB1a but with the addition of a broad, shallow absorbance centered at approximately 285 nm (Figure 3D). This additional absorbance apparently results from an equilibrium mixture of ring-opened aldehyde and hemiacetal (Bull et al., 1984).

Also of use in characterization and identification was the retention time of an unknown residue relative to that of a reference standard. The 8,9-*Z* isomer of an avermectin has been shown to elute immediately after the avermectin in RP HPLC (Maynard, 1989). Therefore, if an unknown residue eluted immediately after a known residue in RP HPLC and its UV absorption spectrum had the characteristic shape of an 8,9-*Z* avermectin (Figure 3B), it could reasonably be suspected as being the 8,9-*Z* isomer of the known residue. Note that in NP HPLC, this relative order of retention times is reversed.

The elution of an unknown as two distinct rotameric peaks

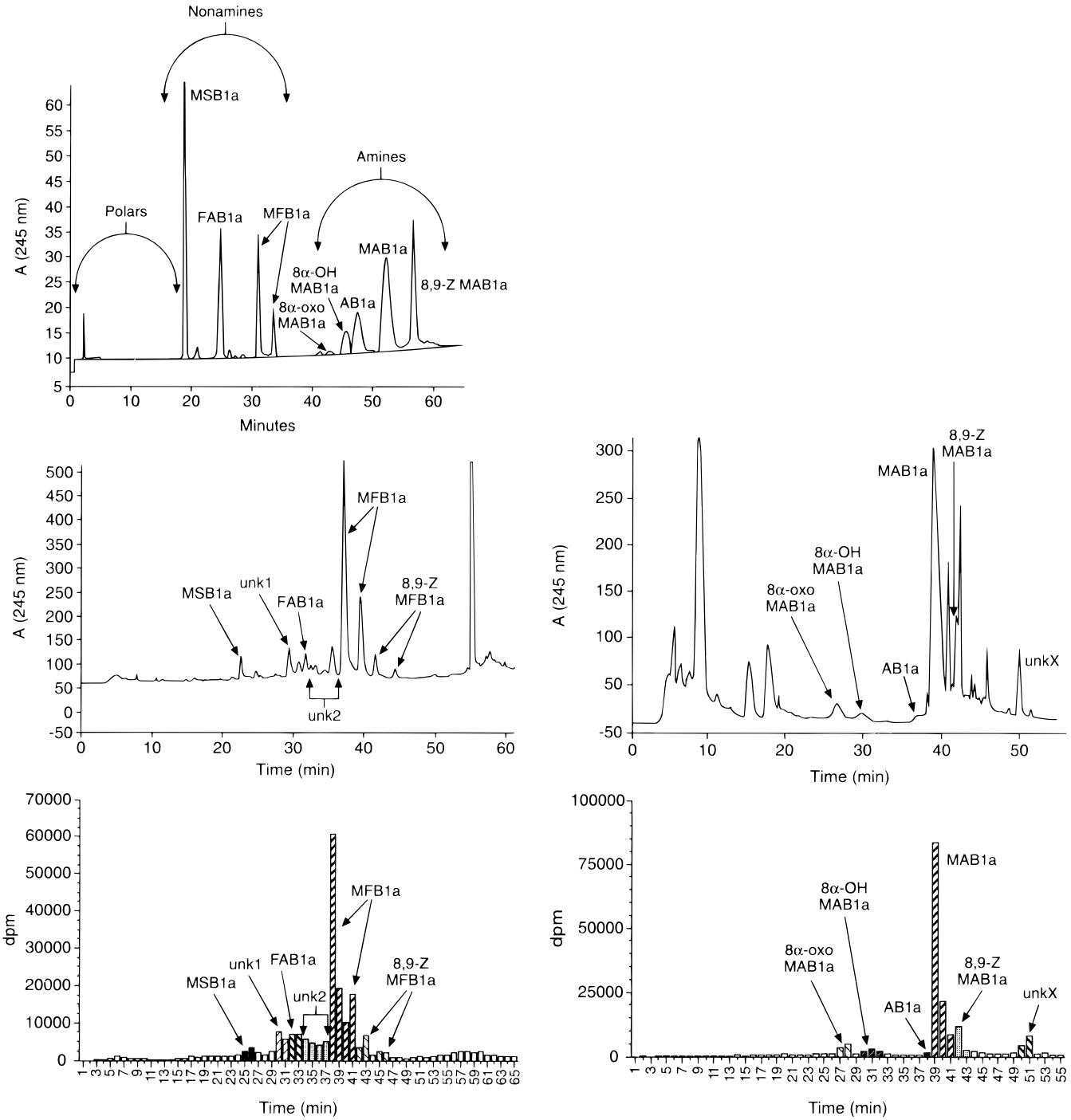

Figure 2. (a, top) Representative C_{18} HPLC chromatogram of MAB1a and related standards (Table 1, method 1B). The elution region designated "polars" is arbitrarily defined as containing all residues eluting before MSB1a. No standards are available for this region. (b, bottom left) C_{18} semipreparative HPLC fractionation (Table 1, method 1A) of the nonamines isolated by C_{18} SPE. The elution profile was divided into six crude residue fractions as shown. Individual residues were isolated from these fractions using a variety of HPLC methods. (c, bottom right) C_{18} semipreparative HPLC fractionation (Table 1, method 2) of the amines isolated by C_{18} SPE. The elution profile was also divided into six crude residue fractions from which individual residues were isolated.

was diagnostic of residues containing an *N*-methyl-*N*-formyl group such as MFB1a. Under all HPLC conditions used in this study MFB1a eluted as two separate peaks representing the two rotamers resulting from hindered rotation about the amide C−N bond. Detection of rotameric peaks by HPLC has previously been reported for other N-substituted amides and thioamides (Boiteux et al., 1984; Lee and Querijero, 1985).

RESULTS

A total of 15 residues (13 radiolabeled and 2 non-radiolabeled) were isolated from the methanol rinse of the surface of cabbage leaves and subsequently identified by either NMR or NMR/MS analysis. Of these, 12 were associated with the nonamine fraction and 3 with the amine fraction. Table 2 details the second- and third-dimension HPLC methods used to isolate each of the residues identified in this study after the initial C_{18} semipreparative HPLC fractionation. Comments relevant to the isolation and identification of some of the individual residues are given below. The structures of all novel residues are presented in Figure 4.

Isolation of Residues from the Nonamine Fraction. *Isolation of 8,9-Z-MSB1a.* This MSB1a isomer was isolated from the C_{18} semipreparative elution region

Table 1. Description of HPLC Methods

method	gradient	conditions[a]
1	80% B to 90% B in 45 min, linearly to 100% B in 5 min, hold for 15 min	A = H_2O, B = MeOH (A) Axxiom ODS semiprep Column 3 mL/min flow rate (B) Axxiom ODS analytical column 1 mL/min flow rate
2	isocratic 87% B for 30 min, linearly to 100% B in 5 min, hold for 15 min	A = H_2O, 5 mM AA B = MeOH, 5mM AA Axxiom ODS semiprep column 3 mL/min flow rate
3	isocratic 93.5% A for 20 min, linearly to 85% A in 15 min, hold for 25 min	A = isooctane, B = EtOH LiChrospher diol column 1 mL/min flow rate (with 0.4 mM TEA for isolation of amines)
4	isocratic 90% A for 30 min, linearly to 77.5% A in 15 min, hold for 10 min	same as method 3
5	isocratic 90% A for 30 min, linearly to 77.5% A in 15 min, hold for 15 min	A = isooctane, 0.4 mM TEA B = ethanol, 0.4 mM TEA LiChrospher diol column 1 mL/min flow rate
6	isocratic 95% A for 20 min, linearly to 85% A in 15 min, hold for 25 min	same as method 5
7	isocratic 40% A for 45 min, linearly to 0% A in 5 min, hold for 10 min	A = H_2O, B = ACN Shiseido Dychrom C_{18} Capcell Pak column 1 mL/min flow rate
8	isocratic 45% A for 45 min, linearly to 0% A in 5 min, hold for 10 min	same as method 7
9	isocratic 45% A for 15 min, linearly to 20% A in 30 min, linearly to 0% A in 10 min, hold for 5 min	same as method 7 (with 0.4 mM TEA for isolation of the amines)
10	isocratic 60% A for 20 min, linearly to 20% A in 20 min, hold for 10 min, linearly to 0% A in 20 min	A = H_2O, B = ACN Zorbax CN column 1 mL/min flow rate

[a] MeOH, methanol; AA, ammonium acetate; ACN, acetonitrile; TEA, triethylamine; H_2O, water; EtOH, ethanol. All gradients are linear. For method 1B, 5 mM AA was used as a modifier for both mobile phases.

Table 2. Summary of Residue Isolation Methods

residue	HPLC methods[a]	μg isolated[b]	% of total[a]	method(s) of structural ID
MSB1a	3	27	0.89	MS, NMR
8,9-*Z*-MSB1a	3, 4	2.6	0.09	NMR
MFB1a	4, 9	106	21.20	NMR, MS
8,9-*Z*-MFB1a	4	60	3.29	NMR, MS
FAB1a	3, 7 and 3, 8	27	1.42	NMR, MS
8α-OH-MFB1a	3, 9, 10, 4	5.2	1.25	NMR
8α-oxo-MFB1a	3, 8	6.4	0.25	NMR
N-methyl-*N*-*cis*-propenal B1a	3, 4	9.7	0.21	NMR, MS
8,9-(*Z*)-*N*-methyl-*N*-*cis*-propenal B1a	4	4	0.16	NMR
oxime	4, 8	116	4.26	NMR
MFB1b	3, 8	ND[d]	ND	NMR
B1a	3, 9	ND	ND	NMR
MAB1a	5, 9	101	14.65	NMR
8,9-*Z*-MAB1a	5, 9	25	1.43	NMR
AB1a	5, 9	12	0.33	NMR

[a] The HPLC methods used in residue isolation after C_{18} semipreparative HPLC fractionation are listed in the order that they were used. See Table 1 for a description of each of these methods. [b] Residue mass (μg of MAB1a benzoate equivalents) isolated and submitted for structural analysis. Does not necessarily represent the total residue mass. [c] Normalized % of total radioactivity in the original methanol rinse sample. [d] ND, not determined.

immediately after MSB1a and before unknown 1 (Figure 2b). A tentative identification was made on the basis of its UV absorption spectrum and its C_{18} retention time relative to MSB1a. The NMR spectrum for this residue is presented in Figure 5.

Isolation of MFB1a. The crude residue fractions containing both MFB1a rotamers from C_{18} semipreparative HPLC (Figure 2b) were combined for further purification and, initially, NMR and MS confirmations were obtained with a small portion of the total MFB1a sample. In the attempt to isolate additional unknown residues from the MFB1a crude residue fraction, one residue, the oxime (see below), was partially resolved from the main MFB1a rotamer (Figure 6). Since the oxime was therefore present in the original sample submitted for NMR, additional MFB1a was isolated and resubmitted for confirmation of structure.

Isolation of 8,9-Z-MFB1a. This residue was initially tentatively identified by its relative retention time on the C_{18} semipreparative column (eluting immediately after MFB1a), by its elution as two apparent rotamers, and by its UV absorption spectrum.

The remaining nonamine residues identified were all isolated from the fractions of the C_{18} semipreparative column beginning immediately before the elution of FAB1a and ending immediately after the elution of the second rotamer of MFB1a (Figure 2b). This region was divided into four fractions (unknown 1, FAB1a, unknown 2, and MFB1a) and was densely populated with avermectin residues (identifiable by the characteristic avermectin UV absorption spectra). Most of these were not present in a large enough quantity to allow for isolation. Figure 6 is the UV chromatogram from NP HPLC analysis of the MFB1a RP semipreparative HPLC fraction and it clearly demonstrates the density of residues in this region. The UV absorption spectra of the individual peaks in this chromatogram as taken by a photodiode array detector are included to demonstrate the characterization of minor residues as avermectins.

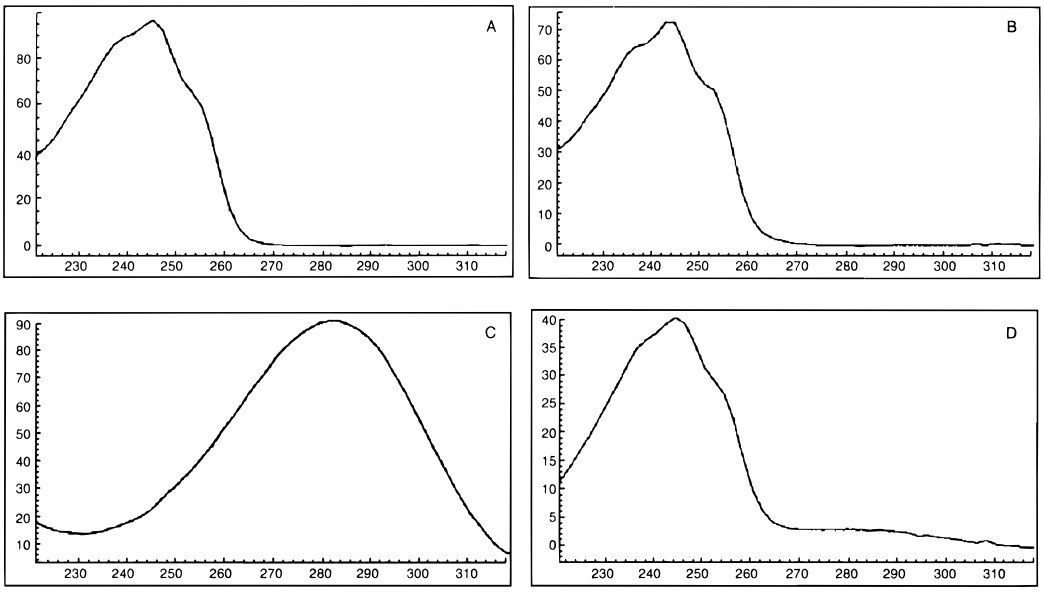

Figure 3. UV absorption spectra (220−320 nm) of (A) MAB1a, (B) 8,9-*Z*-MAB1a, (C) 8α-oxo-MAB1a, and (D) 8α-OH−MAB1a.

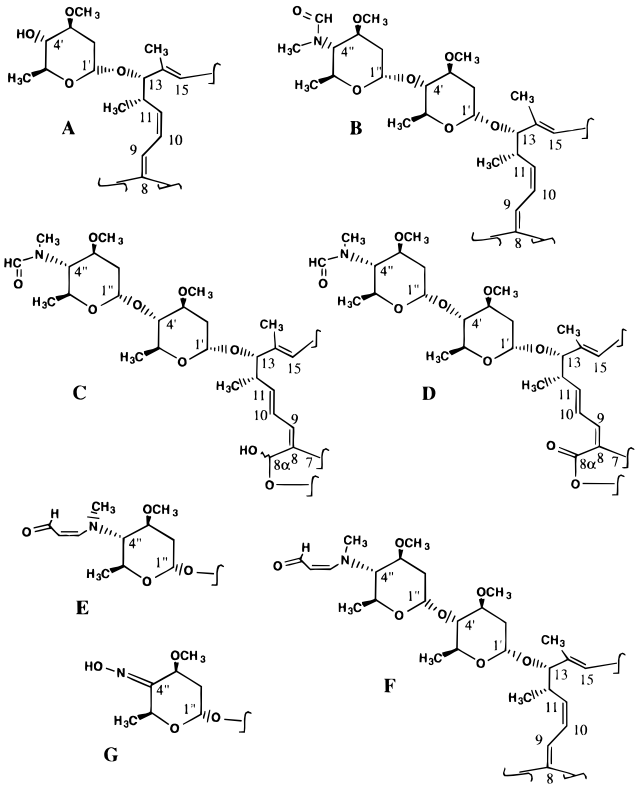

Figure 4. Structures of (A) 8,9-*Z*-MSB1a, (B) 8,9-*Z*-MFB1a, (C) 8α-OH-MFB1a, (D) 8α-oxo-MFB1a, (E) *N*-methyl-*N*-*cis*-propenal B1a, (F) 8,9-(*Z*)-*N*-methyl-*N*-*cis*-propenal B1a, and (G) oxime residues.

Isolation of FAB1a. FAB1a was isolated both from the crude FAB1a fraction and from the unknown 1 fraction.

Isolation of 8α-OH MFB1a. This MFB1a derivative was first isolated from the crude unknown 1 fraction of the C_{18} semipreparative fractionation. A tentative identification was derived from the residue's rotameric elution, which is characteristic of MFB1a derivatives, and from its UV absorption spectrum.

Isolation of 8α-Oxo-MFB1a. This MFB1a derivative was contained in the crude FAB1a fraction from the C_{18} semipreparative column. A tentative identification was made based on its UV absorption spectrum and its rotameric elution.

Isolation of N-Methyl-N-cis-propenal B1a. This unusual residue was isolated from the crude unknown 2 fraction and from the first eluting (major) rotamer of MFB1a. This residue had an unusual UV absorption spectrum (Figure 6, the *N*-methyl-*N*-*cis*-propenal B1a spectrum) in that it exhibited two absorption maxima, one at 245 nm, similar to that of MAB1a, and one at 285 nm resulting from the *N*-propenal group.

Isolation of 8,9-(Z)-N-Methyl-N-cis-propenal B1a. This isomer of the *N*-methyl-*N*-*cis*-propenal B1a residue coeluted with the second rotamer of MFB1a. Its UV absorption spectrum (Figure 6, the 8,9-(*Z*)-*N*-methyl-*N*-*cis*-propenal B1a spectrum) also exhibited two λ_{max}, with one at 245 nm similar to that of 8,9-*Z*-MAB1a and one at 285 nm resulting from the *N*-propenal group. Because it eluted immediately after the *N*-methyl-*N*-*cis*-propenal B1a residue in RP HPLC and because of its spectrum, it was tentatively identified as the 8,9-*Z* isomer the *N*-methyl-*N*-*cis*-propenal residue.

Isolation of Oxime. The oxime coeluted with the major rotamer of MFB1a on both the C_{18} semipreparative column and initially on the diol column. It was only partially resolved from MFB1a with the injection of large amounts of MFB1a (>100 μg) (Figure 6).

Two nonradioactive avermectin residues, the *N*-methyl-*N*-formyl derivative of MAB1b and B1a, were also identified with the nonamine residues. These resulted, respectively, from photolysis of the MAB1b present in the technical grade MK-0244 used for isotopic dilution (the radiolabeled MK-0244 was >97% MAB1a) and from a small amount of B1a possibly present as an impurity in the technical material. MFB1b was first observed during HPLC analysis of the FAB1a fraction, while B1a was first observed during HPLC of the unknown 2 fraction.

Isolation of Residues from the Amine Fraction. The identification of three residues with either an intact methylamine group or a basic amine proton (all corresponding to standards) were obtained by NMR and by comparison with standard retention times. Because of the necessity of using a basic modifier when work is done with the amines, the fractions containing the residue of interest were first extracted into methylene chloride between HPLC isolation steps. This reduced the possibility of breakdown of the base sensitive residues during concentration. However, these precau-

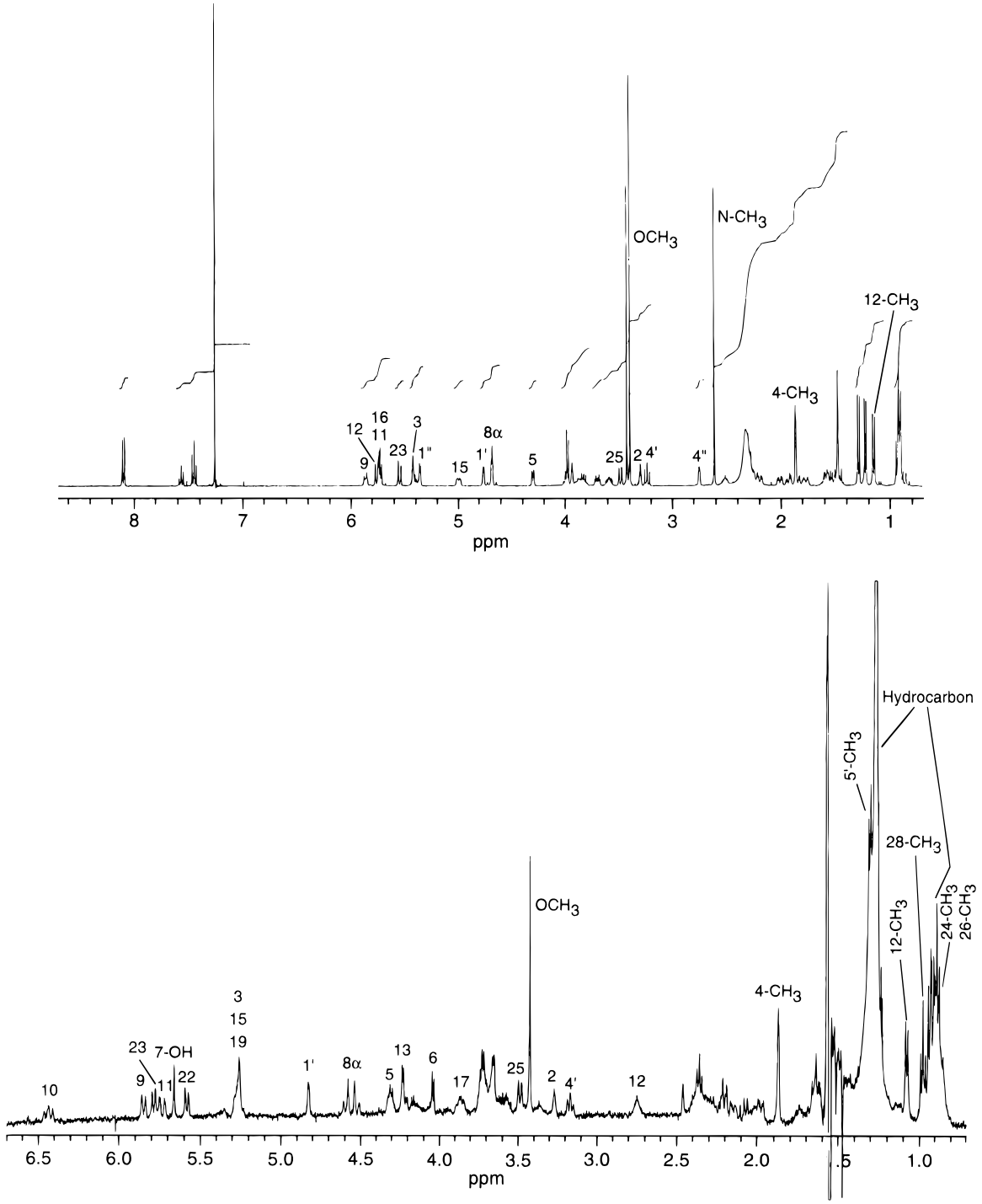

Figure 5. NMR spectrum of MAB1a benzoate at 400 MHz (a, top) and of 8,9-*Z*-MSB1a at 500 MHz (b, bottom). Pertinent signals are labeled.

tions did not prevent the breakdown of 8α-OH-MAB1a and 8α-oxo-MAB1a (tentatively identified from C_{18} semipreparative fractionation of the amines by comparison with standard retention times) during the concentration of the C_{18} semipreparative fractions.

Isolation of Unknown X. This residue had a unique UV absorption spectrum, similar to that of 8,9-(*Z*)-*N*-methyl-*N*-*cis*-propenal B1a (Figure 6) except that the second λ_{max} occurred at 275 nm instead of 285 nm. This residue was submitted for NMR/MS identification but apparently degraded before any meaningful structural information could be obtained.

Nuclear Magnetic Resonance Spectroscopy and Mass Spectrometry. The NMR and MS results for several of these residues have been previously reported (Feely et al., 1992). Only novel results are described here. The proton NMR spectrum of MAB1a standard is shown in Figure 5 as a point of reference with prominent signals labeled.

The 8,9-*Z*-MSB1a residue (Figure 5) was identified by the absence of signals from the outer sugar and by the downfield displacement of H-10 at 6.43 ppm, which is diagnostic of 8,9-*Z* stereochemistry. The relative clarity of the 8,9-*Z*-MSB1a spectrum demonstrates that, with sufficient purity, residues in the 1−5 μg range can be definitively identified by NMR. The 8,9-*Z*-MFB1a residue shows the characteristic 8,9-*Z* downfield displacement of H-10. Also present are pairs of *N*-formyl peaks at 8.13 and 8.19 ppm and pairs of *N*-methyl peaks at 3.09 and 3.15 ppm. The presence of the *N*-methyl-*N*-formyl group in the 8α-OH-MFB1a and the 8α-oxo-

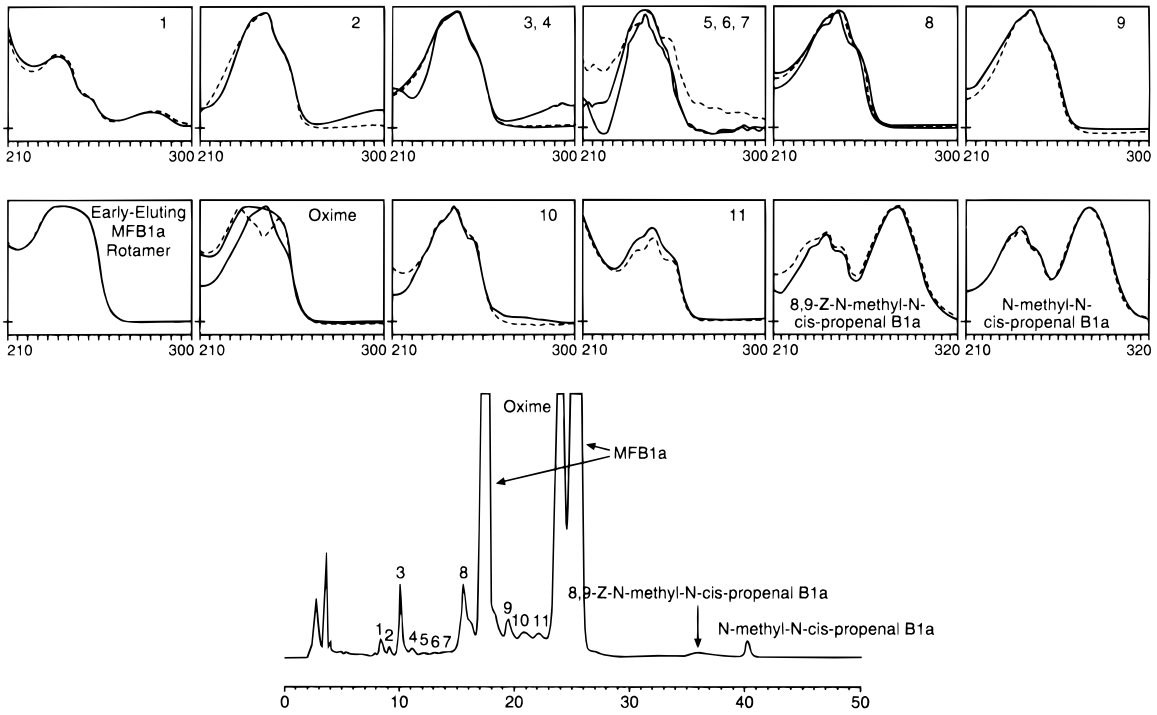

Figure 6. UV chromatogram at 245 nm with associated UV spectra (210−300 nm) from the purification of the MFB1a fraction (Table 1, method 4; see also Figure 2b). Note the double λ_{max} of the *N*-methyl-N-*cis*-propenal and the 8,9-(*Z*)-*N*-methyl-*N*-*cis*-propenal residues. The MFB1a absorption spectrum is misshapen because the amount applied to the column exceeds the linear range of the detector.

MFB1a residues was indicated by these same pairs of signals. The 8α-OH residue exists in an equilibrium between the ring-opened aldehyde and the ring-closed lactol (Bull et al., 1984), and this functionality was recognized by the lack of an 8α-methylene signal and by the presence of two aldehyde peaks at 9.78 and 9.39 ppm. The relative areas of the aldehydic and *N*-formyl protons indicated that approximately 60−65% of the residue was in the aldehyde form. The lactol proton could not be identified with assurance because its predicted chemical shift near 5.6 ppm was in a region of complex signals. For the 8α-oxo residue, extended conjugation displaced the diene protons downfield with H-9 at 6.63 ppm, H-10 at 7.26 ppm, and H-11 at 6.24 ppm. The oxime was identified by the downfield displacement of the 5″-methyl to 1.50 ppm and the 5″-CH to 5.15 ppm. The >1 ppm downfield shift of the 5″-H and the absence of a 4″-H signal indicated the conversion of the 4″-C to sp^2. The 4″-keto analogue was excluded by comparison with a model compound. For the *N*-methyl-*N*-*cis*-propenal B1a residue and its 8,9-*Z* stereoisomer, the presence of the propenal group and its *cis* stereochemistry were inferred by signals at 9.13, 7.53, and 5.23 ppm. The attachment of this group to nitrogen was inferred from the downfield displacement of the *N*-methyl group and the 4″-H.

FAB-MS analysis of the *cis*-propenal residue indicated the expected molecular formula of $C_{52}H_{77}NO_{14}$, which is C_3H_2O more than MAB1a ($C_{49}H_{75}NO_{13}$). EI-MS analysis confirmed that the aglycon moiety was unchanged and that the terminal sugar had been modified.

DISCUSSION

The residue profile for the experimental pesticide MK-0244 on the surface of cabbage leaf is qualitatively similar to that seen after photolysis of MAB1a thin films on glass (Feely et al., 1992). Residues identified from both cabbage leaf and from photolysis on glass include MSB1a, FAB1a, MFB1a, AB1a, 8,9-*Z*-MAB1a, and parent. However, the relative proportions of the degradates are different. The five main residues isolated from thin film photolysis on glass (16 h of UV exposure) in order of abundance were parent, AB1a, 8,9-*Z*-MAB1a, FAB1a, and MFB1a (Feely et al., 1992). The five major residues isolated from a methanol rinse of the cabbage surface were MFB1a, parent, the oxime, 8,9-*Z*-MFB1a, and 8,9-*Z*-MAB1a.

Seven residues (8,9-*Z*-MSB1a, 8,9-*Z*-MFB1a, 8α-OH-MFB1a, 8α-oxo-MFB1a, *N*-methyl-*N*-*cis*-propenal B1a, 8,9-*Z*-*N*-methyl-*N*-*cis*-propenal B1a, and the oxime) were identified or tentatively identified from the cabbage leaf rinse but not from photolysis on glass (Feely et al., 1992). Three residues (8,9-*Z*-FAB1a, 8,9-*Z*-AB1a, and Δ-2,3-MAB1a) were identified from the photolysis on glass but not on cabbage leaf. However, except for *N*-methyl-*N*-*cis*-propenal B1a, 8,9-(*Z*)-*N*-methyl-*N*-*cis*-propenal B1a, and possibly the oxime, none of these is believed to be exclusively associated with photolysis on glass or on cabbage. For example, photoisomerization of the 8,9 double bond appears to be a readily available reaction pathway for avermectins (Crouch et al., 1991; Feely et al., 1992; Moye et al., 1990; Mrozik et al., 1988). It can thus be argued that four of the 8,9-*Z* isomers that were not identified as common to both studies (the 8,9-*Z* of MSB1a, FAB1a, MFB1a, and AB1a) were nonetheless present as minor residues in both studies but were not isolated. Also, as the oxime coelutes with the main rotamer of MFB1a under at least two HPLC conditions, it can be speculated that if it had been produced in relatively minor amounts during photolysis on glass, it would probably not have been isolated from MFB1a and it would probably not have interfered with subsequent structural analysis of MFB1a.

Feely et al. (1992) concluded that the 4″-methylamino group of MAB1a was the "region most sensitive to photodegradation" in the photolysis of MAB1a thin films. Because 7 of the 13 residues identified have changes to the 4″-methylamino group and because the

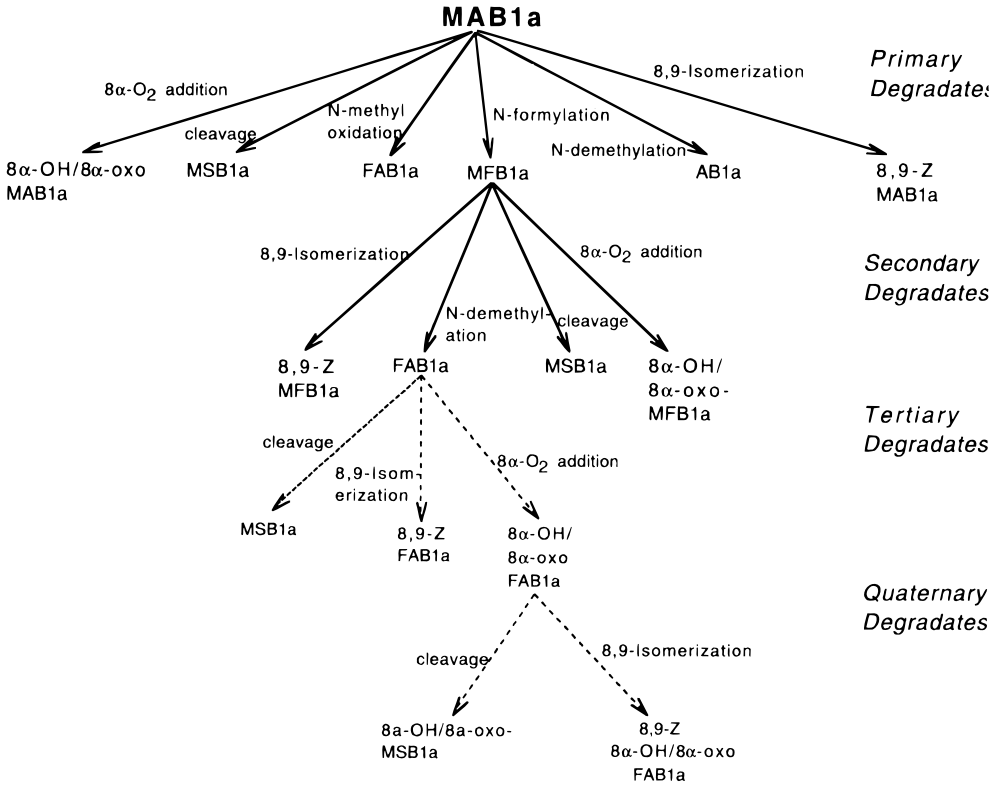

Figure 7. MAB1a and related residues undergo at least six transformations: 8,9-isomerization, N-demethylation, *N*-methyl oxidation, N-formylation, cleavage of the outer sugar, and addition of oxygen to the C-8α position leading to 8α-oxo-MAB1a and 8α-OH-MAB1a. Because these transformations are apparently available to all avermectin-like residues (unless excluded by lack of functionality, i.e., MSB1a cannot undergo N-demethylation), the resulting residue profile is extremely complex. In each step of the degradation pathway shown (primary, secondary, etc.), the scheme focuses on the transformations of a single residue. A total of 32 residues are possible in this scheme.

predominant residue seen is MFB1a, the 4″-methylamino group is also the major site of transformation in MK-0244 on cabbage.

It is therefore clear that MK-0244 degradation on the surface of cabbage results mainly from photolysis and not from plant metabolism. Transformations common to the photodegradation of MK-0244 as a thin film on glass and on the surface of cabbage leaf are photoisomerization of the 8,9 double bond, *N*-methyl to *N*-formyl oxidation, N-demethylation, N-formylation (or N-methylation of FAB1a), loss of the outer sugar, addition of oxygen to the 8α position, and perhaps formation of the oxime (see Figure 7).

Some of these transformations appear to result from either singlet oxygen or free radical reactions. Previously observed amine−singlet oxygen reactions include N-demethylation (Lindner et al., 1972) and *N*-methyl to *N*-formyl oxidation (Fisch et al., 1971). It has been noted (Fisher and Mrozik, 1989) that the C-8α position of an avermectin is both allylic and α to an ether linkage, making it susceptible to radical reactions. Crouch et al. (1991) postulated that a radical reaction between oxygen and the 8α position of avermectin B1a initially forms a hydroperoxide which then either loses water to form the ketone (8α-oxo-MAB1a) or is photolytically cleaved to form the allylic alcohol (8α-OH-MAB1a). Feely et al. (1992) postulated that the monosaccharide could be formed by simple cleavage of the ether linkage to the free radical, which would then abstract a hydrogen to form the product.

At present there is no convincing mechanism to explain the formation of the *N*-methyl-*N*-formyl residue. Two possibilities would be N-formylation of MAB1a and N-methylation of FAB1a. There are a number of studies describing *N*-formyl metabolites of basic and nonbasic amines in mammals (Abbott et al., 1990), but this would apparently be a unique photochemical transformation. Free radical alkylations of basic nitrogens have also been reported (Augusto, 1993), but the source of the putative methyl radical needed to convert FAB1a to MFB1a is unknown.

Metabolic conversion of primary and secondary amines to oximes through hydroxyamine intermediaries has been previously demonstrated in mammals (Abbott et al., 1990; Clement et al., 1993; Hucker, 1973; Parli et al., 1971) and in fungi (Foster et al., 1989). However, there are apparently no reported examples of the photochemical conversion of an amine to an oxime.

Also, the source of the three-carbon fragment in *N*-methyl-*N*-*cis*-propenal B1a is unknown, though it is informative to observe that this residue undergoes 8,9-*Z* isomerization. It was initially hypothesized that the source of this fragment was either the polycarbonate spray bottle used in application or the polyethylene sample storage bottle. However, when a methanol solution of MK-0244 standard was stored at room temperature in both bottle types for extended periods of time, no similar residue was seen (data not shown).

In addition to the [^{14}C]MAB1a degradates found, two nonradioactive residues were identified by NMR: B1a and MFB1b. Also, nonradioactive MAB1b was tentatively identified by HPLC retention time relative to MAB1a standard, but it was not submitted for NMR confirmation of structure. The B1a residue is presumably a contaminant present in the MK-0244 technical grade material used to dilute the [^{14}C]MAB1a. This is understandable since the semisynthetic MAB1a is made directly from B1a. The MFB1b obviously results from photodegradation of the approximately 10% MAB1b present in the technical grade material as the photo-

degradation of the two homologues has been shown to be similar (Wrzesinski, unpublished data).

In this study nine primary degradates and five secondary degradates of MAB1a were identified or tentatively identified. Considering only the 6 primary residue processes delineated in Figure 7, a total of 32 unique residues are possible. However, besides the residues identified as described above, there were numerous additional avermectin-like residues (as determined by UV absorption spectra) which were not present in sufficient quantities for structural identification. For example, considerable complexity of residues was encountered during purification of MFB1a (Figure 6). Although MFB1a and the oxime were clearly the main residues present, there were also many minor residues that possessed characteristic avermectin-like absorption spectra but which were not present in sufficient quantity for identification (as demonstrated by unknown residues 2−11 in Figure 6). The abundance of these residues suggests, first of all, that there are likely a number of other degradation pathways open to MK-0244 which have not yet been defined. It also suggests a possible source for the polar residues (polars) mentioned above and found in all previous photolysis and plant metabolism studies of MAB1a and B1a (Crouch et al., 1991; Feely et al., 1992; Moye et al., 1990).

These polar degradates of avermectins appear to consist of numerous minor residues which, because of their sheer numbers, are not easily individually isolated and which lack the characteristic avermectin UV absorption spectra (Maynard et al., 1989). Time course photolysis studies have indicated that while polar degradates begin to form almost immediately and, with extended photolysis, predominate, it is the avermectin-like residues that initially predominate (Crouch et al., 1991; Feely et al., 1992). As detailed above and in Figure 7, a total of 32 avermectin-like residues can be generated from the 6 degradation processes. If the polar degradates were generated only from these residues by a single mechanism, they would total 64 residues. It is quite clear that all of the photodegradation pathways for MAB1a have not been elucidated, and it is probable that there is more than a single reaction pathway leading to formation of the polar degradates. Therefore, the total number of polar residues would be expected to be extremely large.

The work presented here demonstrates a definite parallel between the photodegradation of MAB1a on glass and the degradation of MK-0244 on the surface of cabbage. It also illustrates the complexity of the MK-0244 plant residue profile. Further studies of the fate of MK-0244 in cabbage will be presented in subsequent papers including the nature of the entire extractable residue and the bound residue in plants treated with multiple applications of [^{3}H/^{14}C]MK-0244.

ACKNOWLEDGMENT

We thank William F. Feely for advice and assistance with the isolation and initial characterization of residues.

LITERATURE CITED

Abbott, F. S.; Slatter, J. G.; Burton, R. Identification of biliary metabolites of (±)-3-dimethylamino-1,1-diphenylbutane HCl (Recipavrin) in rats. *Xenobiotica* **1990**, *20* (10), 999.

Augusto, O. Alkylation and cleavage of DNA by carbon-centered radical metabolites. *Free Radical Biol. Med.* **1993,** *15* (3), 329.

Boiteux, S.; Belleney, J.; Roques, B. P.; Laval, J. Two rotameric forms of open ring 7-methylguanine are present in alkylated polynucleotides. *Nucleic Acids Res.* **1984**, *12* (13), 5429.

Bull, D. L.; Ivie, G. W.; MacConnell, J. G.; Gruber, V. F.; Ku, C. C.; Arison, B. H.; Stevenson, J. M.; VandenHeuval, W. J. A. Fate of avermectin B1a in soil and plants. *J. Agric. Food Chem.* **1984**, *32*, 94−102.

Clement, B.; Lustig, K.; Ziegler, D. M. Oxidation of desmethylpromethazine catalyzed by pig liver flavin-containing monooxygenase. Number and nature of metabolites. *Drug Metab. Dispos.* **1993**, *21* (1), 1993.

Crouch, L.; Feely, W.; Arison, B.; VandenHeuvel, W.; Colwell, L.; Stearns, R.; Kline, W.; Wislocki, P. Photodegradation of avermectin B1a thin films on glass. *J. Agric. Food Chem.* **1991**, *39*, 1310.

Feely, W.; Crouch, L.; Arison, B.; VandenHeuvel, W.; Colwell, L.; Wislocki, P. Photodegradation of 4′-(Epimethylamino)-4′-deoxyavermectin B_{1a} thin films on glass. *J. Agric. Food Chem.* **1992**, *40*, 691.

Fisch, M.; Gramain, J.; Oleswn, J. Photo-oxidation of amines: a reply. *Chem. Commun.* **1971**, 663.

Fisher, M.; Mrozik, H. Chemistry. In *Ivermectin and Abamectin*; Campbell, W. C., Ed.; Springer-Verlag: New York, 1989; Vol. 1, Chapter 1.

Foster, B. C.; Coutts, R. T.; Pasutto, F. M. Biotransformation of aryl alkylamines by *Cunninghamella bainieri*. *Xenobiotica* **1989**, *19* (5), 531.

Hucker, Howard B. Phenylacetone oxime—an intermediate in amphetamine deamination. *Drug Metab. Dispos.* **1973**, *1*, 332.

Ku, C. C.; Hwang, S. C.; Kaplan, L.; Nallin, M. K.; Jacob, T. A. The preparation of carbon-14 labeled avermectin B1a. *J. Labelled Compd. Radiopharm.* **1984**, *22* (5), 451.

Lee, H. K.; Querijero, G. Kinetics and mechanisms of thioamide rotational isomerism: *N*-thionaphthoyl-*N*-methyl glycine derivative. *J. Pharm. Sci.* **1985**, *74* (3), 273.

Lindner, J.; Kuhn, H.; Gollnick, K. Demethylation of codeine to norcodein by Sensitized photooxygation. *Tetrahedron Lett.* **1972**, *17*, 1705.

Maynard, M.; Maynard, H. HPLC Assay for avermectin B_{1a} and its two photoisomers using a photo diode array detector. *Bull. Environ. Contam. Toxicol.* **1989**, *43*, 499.

Moye, H.; Malagodi, M.; Yoh, J.; Deyrup, C.; Chang, S.; Leibee, G.; Ku, C.; Wislocki, P. Avermectin B_{1a} metabolism in celery: a residue study. *J. Agric. Food Chem.* **1990**, *38*, 290.

Mrozik, H.; Eskola, P.; Reynolds, G.; Arison, B.; Smith, G.; Fisher, M. Photoisomers of avermectins. *J. Org. Chem.* **1988**, *53*, 1820.

Parli, John C.; Wang, Nancy; McMahon, E. The enzymatic *N*-hydroxylation of an imine. A new cytochrome P-450-dependant reaction catalyzed by hepatic microsomal monooxygenases. *J. Biol. Chem.* **1971**, *246* (22), 6953.

Received for review January 6, 1995. Revised manuscript received May 11, 1995. Accepted October 6, 1995.[⊗]

JF9500142

[⊗] Abstract published in *Advance ACS Abstracts,* December 15, 1995.